Composition of Hydrofullerene Mixtures Produced by C_{60} Reaction with Hydrogen Gas Revealed by High-Resolution Mass Spectrometry

Alexander V. Talyzin,*,† Yury O. Tsybin,‡ Tanner M. Schaub,‡ Philippe Mauron,§ Yury M. Shulga,|| Andreas Züttel,§ Bertil Sundqvist,† and Alan G. Marshall‡

Department of Physics, Umeå University, 901 87 Umeå, Sweden, Ion Cyclotron Resonance Program, National High Magnetic Field Laboratory, Tallahassee, Florida 32310-4005, Physics Department, Fribourg University, Pérolles, CH-1700 Fribourg, Switzerland, and Institute of Problems of Chemical Physics, RAN, 142432, Chernogolovka, Moscow Region, Russia

Received: April 4, 2005; In Final Form: May 12, 2005

Complex solid hydrofulleride mixtures were synthesized by prolonged hydrogenation of C_{60} at 120 bar hydrogen pressure, 673 K temperature, and different reaction periods. The high degree of hydrogenation was confirmed by infrared spectroscopy and X-ray diffraction. The identity of hydrogenation products was determined by high-resolution field desorption/ionization Fourier transform ion cyclotron resonance mass spectrometry. Despite partial gas-phase fragmentation of hydrofullerene ions during mass analysis, the data suggest that the synthesized mixtures consist of mostly $C_{58-60}H_x$ hydrofullerenes. Increasing the duration of hydrogenation results in synthesis of $C_{59}H_x$ and $C_{58}H_x$ as major products. Possible hydrofullerene fragmentation pathways during both material synthesis and mass spectrometric analysis are discussed. Gas-phase fragmentation in the mass spectrometer arises from hydrofullerene ions $C_{60}H_x^+$ with $x > 40$ and $C_{59}H_{44}^+$ with drastically decreased molecular stability relative to the known $C_{60}H_{36}$.

Introduction

Fullerenes with small numbers of carbon atoms (<60) have been predicted to have rather unusual properties, including room-temperature superconductivity upon doping with alkali metals.[1] It has recently been suggested that small hydrogenated fullerenes (for example, $C_{28}H_4$) could preserve superconductivity at high temperature.[2] Although curvature stress effects make small fullerenes unstable, hydrogen or chlorine bond termination can provide additional molecular stability.[3,4] Small fullerenes remain largely unstudied and only single reports are known for synthesis of a few mg of these samples.[3,4] Controlled fragmentation of C_{60} provides a means to synthesize bulk quantities of these novel materials. The collapse of bulk amounts of C_{60} can be achieved by several methods, for example, by treatment at high temperature and pressure;[5] however, this method transforms the fullerene into graphite or amorphous carbon. Stabilization is required to achieve controlled collapse of the fullerene cage structure, and hydrogenated C_{60} may be an advantageous starting material for fragmentation.

Relatively pure hydrofullerides, $C_{60}H_{36}$ and $C_{60}H_{18}$, are well-known and can be produced by several reactions such as the Birch reduction, transfer hydrogenation with 9,10-dihydroanthracene, and so forth.[6−11] Characterization of hydrofullerides by X-ray diffraction (XRD) and various spectroscopic methods[12−14] has been performed but remains difficult because of the large number of possible isomers for each hydrofulleride composition. Direct reaction of fullerenes with hydrogen gas requires elevated temperature (~573−673 K) and a hydrogen pressure of 50−120 bar and yields mixtures of hydrofullerides with different composition.[15−18] The maximum overall hydrogen content achieved under prolonged hydrogenation (at 673 K and 120 bar H_2) is ~5 wt %.[19] During hydrogenation, the sample weight increases for some time by addition of hydrogen, followed by a decrease in sample weight as the cage structure begins to collapse. We recently showed that the final products of C_{60} collapse are likely polycyclic aromatic hydrocarbons (PAH).[19−21] Because of stabilization with hydrogen, formation of graphite or amorphous carbon is avoided and large fragments of C_{60} survive the treatment intact.[20,21] Although unusual hydrocarbon molecules themselves are interesting, we focus here on intermediate products between hydrogenated C_{60} and PAH, namely, hydrogenated fullerenes with smaller cage structure (fragmented fullerenes).

Our prior low-resolution matrix-assisted laser desorption ionization time-of-flight mass spectrometry (MALDI TOF MS) and high-resolution field desorption/ionization Fourier transform ion cyclotron resonance mass spectrometry (FD FT-ICR MS) suggested that controlled fragmentation of C_{60} leads primarily to synthesis of the fragmented fullerenes, $C_{59}H_x$ and $C_{58}H_x$.[20,21] The analytical advantage of FD FT-ICR MS for this analysis was demonstrated by resolving and identifying signals from ions of the same nominal molecular mass (for example, $C_{59}H_{28}^+$ and $C_{60}H_{40}^+$). That capability, combined with the high mass accuracy provided by internal spectral calibration, enabled elemental composition assignment for complex mixtures of $C_{60}H_x^+$ and ions of fragmented hydrofullerenes.[22,23]

However, in that analysis, some gas-phase fragmentation of unstable hydrofullerene ions was observed as well. The fragmentation mechanism responsible for fragmentation of hydrogenated fullerene ions during FD FT-ICR MS could be similar to the previously observed ejection of C_2 units during electron impact and ion bombardment of C_{60}.[24−27] Therefore, we now report detailed characterization of the products of prolonged C_{60} hydrogenation and fragmentation (at elevated temperature and

* To whom correspondence should be addressed. E-mail: alexandr.talyzin@physics.umu.se.
† Umeå University.
‡ National High Magnetic Field Laboratory.
§ Fribourg University.
|| Institute of Problems of Chemical Physics.

10.1021/jp051707g CCC: $30.25 © 2005 American Chemical Society
Published on Web 06/15/2005

H_2 pressure) by high-resolution FD FT-ICR MS and complementary XRD and IR spectroscopy. We discuss gas-phase fragmentation of labile hydrofullerene ions during FD FT-ICR MS, possible fragmentation pathways, and sources of fragmentation.

Experimental Section

C_{60} (99.5% pure, MTR Ltd., Cleveland, OH) was typically loaded at 0.5−1 g. Hydrogenation at 120 bar H_2 gas pressure, 673 K was performed for 1300 min (sample 1) and 3000 min (sample 2). The treatment period for the first sample corresponded to the saturation point in hydrogen addition,[19] whereas sample 2 was treated longer to produce more fragmentation, however, not as long as investigated previously (i.e., 4300 min[19,20]), to avoid accumulation of cage collapse products. Prior to hydrogenation, samples were degassed by heating at 473 K in a vacuum (10^{-5} Torr) for several hours. In contrast to previous experiments,[19,20] the hydrogenation was performed with a simplified apparatus consisting of a sealed volume and static hydrogen atmosphere. Prior to mass analysis, the samples were dissolved in toluene to a concentration of 0.01−0.1 mg/mL and 20−40 nL of that solution and was loaded onto the field desorption emitter in the ion source of the mass spectrometer for each measurement.

IR spectra were collected with a Perkin-Elmer Spectrum BX-II spectrometer for a sample pressed in a KBr pellet. The X-ray powder diffraction analysis was performed by use of the Cu Kα line from a Philips powder diffraction system with a PW1820 goniometer.

FT-ICR mass spectrometry was performed with a home-built 9.4 T FT-ICR mass spectrometer equipped with a field desorption ion source described elsewhere.[23] In the field desorption/ionization process, positive ions are formed by electron detachment from the molecule and by electron tunneling through a potential barrier whose magnitude is drastically reduced by application of a strong external electrical field. A sample solution is applied to the field desorption emitter (consisting of carbon microneedle dendrites grown on the surface of a 10-μm diameter tungsten filament) in vacuo, and the solvent is allowed to evaporate prior to application of the ionizing electric field. To assist desorption/ionization, the emitter is resistively heated by 10−60 mA current. Following ionization, ions are collected for 10−30 s in a linear octopole ion trap that employs helium bath gas (~1 mTorr) for collisional cooling. The ion packet is then transferred from the accumulation octopole through the magnetic field gradient to an open cylindrical Penning ion trap at magnetic field center.[23] Trapped ions are cooled by a helium gas pulse prior to ICR excitation/detection. Single scan mass spectra for each sample were internally calibrated, and elemental composition assignments were based on accurate mass measurement and Kendrick sorting.[21,22]

Results and Discussion

X-ray Diffraction and IR Spectroscopy. Prior to mass spectrometry, the hydrogenated samples were analyzed by powder XRD (Figure 1) and IR spectroscopy (Figure 2). Under normal conditions (room temperature, atmospheric pressure), the C_{60} crystal structure is face-centered cubic (FCC) with cell parameter $a = 14.17$ Å.[28] The structure of highly hydrogenated C_{60} could remain FCC, but the cell parameter increases to $a =$ 15.0−15.2 Å. In some reports, the structure became body-centered cubic (BCC) in highly hydrogenated samples.[29,30] The volume per C_{60} molecule calculated from cell parameters is almost exactly the same for both FCC and BCC structures of highly hydrogenated C_{60}. Therefore, both structures contain

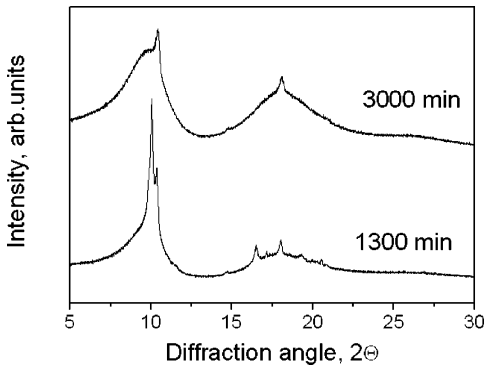

Figure 1. X-ray powder diffraction patterns of samples hydrogenated for 1300 and 3000 min at 673 K and 120 bar H_2 pressure (without hydrogen flow).

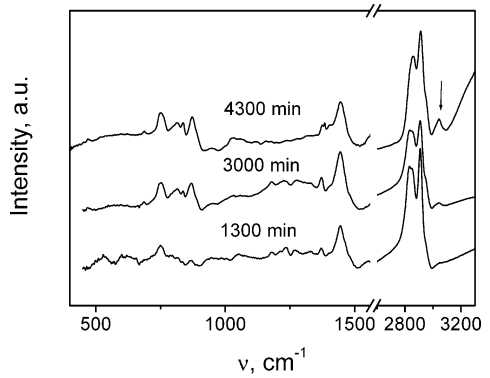

Figure 2. IR spectra of samples hydrogenated for 1300 and 3000 min without hydrogen flow. The IR spectrum of the sample hydrogenated for 4300 min at the same P−T conditions but with hydrogen flow is added from reference 20.

molecules with a similar degree of hydrogenation but packed differently. The increase in cell volume per C_{60} molecule can be calibrated against hydrogen content, on the basis of our previous XRD study.[19]

XRD data reveal that the sample heated for 1300 min is mostly crystalline with FCC structure and cell parameter $a =$ 15.2 Å, with a small fraction of BCC phase (12.05 Å). The cell volumes per molecule calculated from those cell parameters are almost the same: 878 Å^3/molecule for FCC and 875 Å^3/molecule for BCC. According to our previous calibration, those values correspond to an overall hydrogen content of ~5 wt %.[19] The sample heated for 3000 min shows only three peaks from the BCC structure ($a = 12.05$ Å) and some very broad background features. This change in XRD is certainly connected to an increased degree of hydrogenation, which results in more extensive structure disorder. That disorder could arise from partial collapse of hydrofullerene molecules and accumulation of various hydrocarbon molecules resulting from that collapse. The broad peaks are also markedly downshifted, reflecting an increase in unit cell volume. It is rather remarkable that this disorder affects mostly the FCC structure, whereas the BCC peaks remain sharp even in the sample with a longer hydrogenation period.

Further evidence for significant changes in composition of samples subjected to prolonged hydrogenation can be inferred from the infrared (IR) spectra (Figure 2). The IR spectra of hydrogenated fullerenes exhibit peaks in two spectral regions: cage vibrations (<1500 cm^{-1}) and a second region typical of C−H vibrations of hydrogenated C_{60} (~2700−3000 cm^{-1}). Some broad weaker peaks centered approximately at 3015 and 3043 cm^{-1} (Sample 2) are found in the spectral region typical of valence C−H vibrations of aromatic compounds and poly-

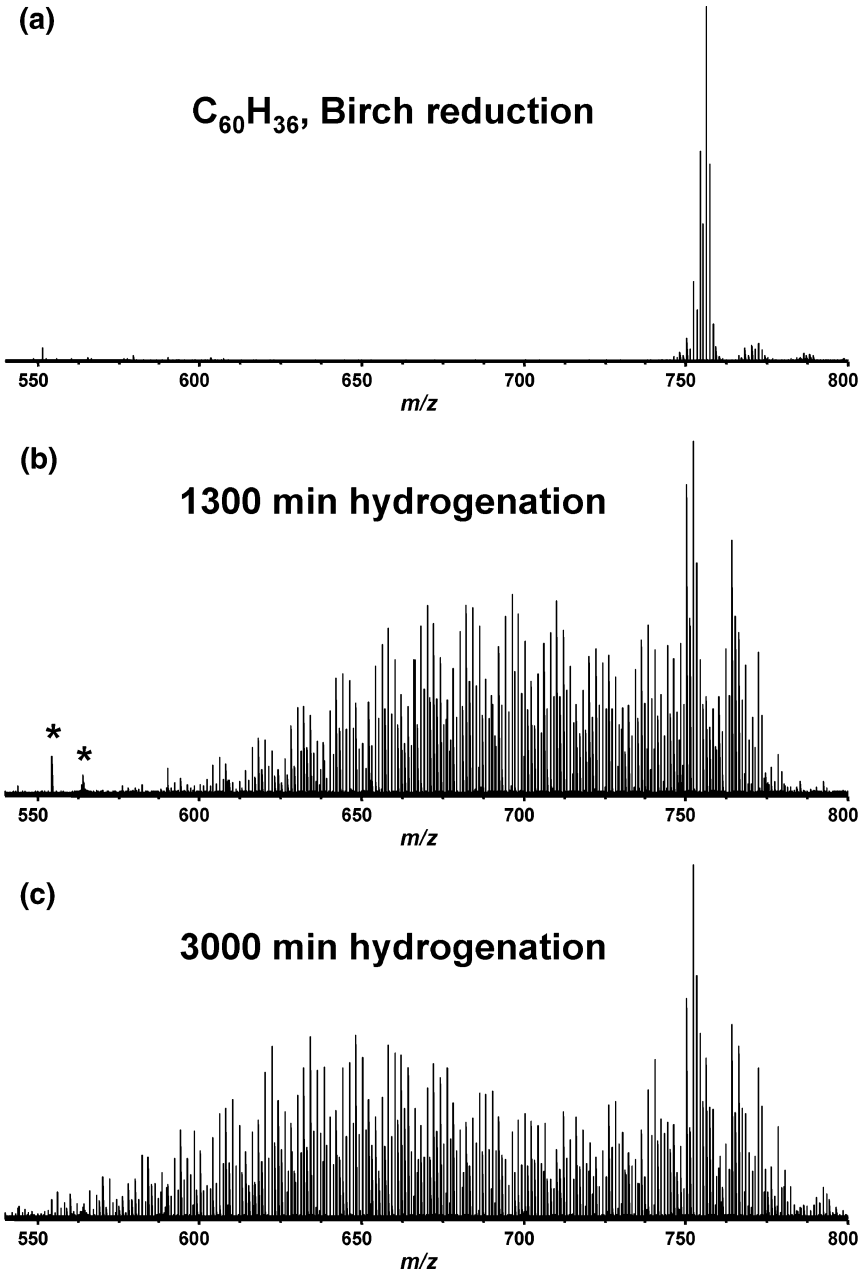

Figure 3. FD FT-ICR mass spectra recorded under the same experimental conditions. (a) Mass spectrum of the sample of mostly $C_{60}H_{36}$ synthesized by Birch reduction; (b) mass spectrum after 1300 min hydrogenation; and (c) mass spectrum after 3000 min hydrogenation. Asterisks (∗) denote electronic noise peaks.

cyclic aromatic hydrocarbons (PAH). Those peaks are consistent with partial collapse of cage structure with formation of relatively large hydrocarbon fragments of $C_{60}H_x$.[19] Figure 2 clearly shows that the amount of PAH material is higher in the more hydrogenated sample, whereas Sample 1 shows it only as minor impurity.

Analysis of C−H vibrations of the fullerenes reveals only some relative change in intensity of the main modes between three samples. The region of cage vibrations of the fullerene molecule shows much more pronounced differences. Several new peaks can be recognized in IR spectra of samples hydrogenated for 1300 min (sample 1) and 3000 min (sample 2). Many of those peaks are not resolved, presumably because of heterogeneous composition. Those IR spectral peaks do not match those for any known $C_{60}H_x$ molecules. Moreover, the presence of $C_{59}H_x$ or $C_{58}H_x$ cannot be confirmed, because their IR spectra have never been studied experimentally or theoretically. Nevertheless, it is clear from the spectra in Figure 2 that most of the sample is composed of hydrofullerenes that retain their cage structure and that prolonged hydrogenation results in profound changes of sample composition.

High-Resolution FD FT-ICR Mass Spectrometry. Field desorption FT-ICR MS of pure fullerene molecules (C_{60}) generates a mass spectrum having the isotopic distribution of C_{60} with no observed fragmentation, even at prolonged ion accumulation intervals and high FD emitter temperature.[22] The mass resolving power is typically very high ($50\,000 < m/\Delta m_{50\%} < 500\,000$) and mass accuracy is better than 1 ppm. The efficiency of hydrogenated fullerene ionization by field desorption/ionization is comparable to that obtained by matrix assisted laser desorption/ionization (MALDI) and exceeds the ionization efficiency achieved by electrospray ionization (ESI).

The FD FT-ICR mass spectrum of C_{60} modified by Birch reduction (to produce mostly $C_{60}H_{36}$) does not exhibit fragmentation (Figure 3a). The FD FT-ICR mass spectra of the hydrogenated samples (sample 1 and sample 2) exhibit many

peaks below *m/z* 720 (i.e., C_{60}) that indicate fragmentation of hydrofullerene molecules (Figure 3b, c). The three spectra shown in Figure 3 were collected under identical instrumental conditions. Longer hydrogenation period (Figure 3c compared to Figure 3b) leads to more extensive reactions and fragmentation.

Although some fragmentation during synthesis (with formation of $C_{55-59}H_x$) was expected,[19−21] the long series of fragmentation products seen in Figure 3 are most likely formed during FD FT-ICR analysis because of the relatively unstable nature of the hydrogenated fullerenes. Indeed, in FD FT-ICR mass spectrometry, fragmentation can result from field-induced reactions of the liquid sample at the emitter surface, thermal decomposition induced by heating of the FD emitter, ion−neutral/ion−ion interactions during external ion accumulation, and instability of the internally excited radical molecular cation formed by field desorption.[23] Therefore, analysis of the FD FT-ICR mass spectra of the hydrogenated fullerene samples is somewhat complicated by products of two different fragmentation mechanisms: hydrofullerene fragmentation during sample preparation and hydrofullerene ion fragmentation during analysis. Labile species in the hydrogenated samples but not in the $C_{60}H_{36}$ reference sample (Birch reduction) may be $C_{60}H_x$ hydrofullerene ions ($X > 40$) or ions of fragmented fullerenes (such as $C_{59}H_{44}^+$).

Furthermore, highly hydrogenated C_{60} species are typically not observed in samples produced by various chemical reduction methods, and their stability decreases with increased hydrogenation.[14] On the other hand, $C_{59}H_x$ is expected to be less stable for geometrical reasons. Taking away one carbon atom from the C_{60} structure leaves a dangling bond (saturated by hydrogen) and a "hole" in the cage structure. The high-resolution data obtained by FD FT-ICR MS afford direct analysis of these possibilities.

Sample Composition. The primary advantage of FD FT-ICR MS for the analysis of complex mixtures of hydrofullerenes is the ability to assign elemental compositions on the basis of accurate mass measurement of ion signals not resolved by other mass analyzers. For example, ion signals from complex hydrofullerene mixtures obtained by time-of-flight mass spectrometry (TOF MS) could be assigned to numerous hydrofullerene species (e.g., a peak at $m/z = 748$ could originate from $C_{60}H_{28}^+$, $C_{59}H_{40}^+$, or $C_{58}H_{52}^+$). In Figure 4, *m/z* scale-expanded segments of the FD FT-ICR mass spectra illustrate the resolved ion signals from those compounds and the corresponding elemental composition assignments on the basis of accurate mass measurement. The full elemental composition assignments for both samples are shown in Figure 5.

Although some observed species were likely produced during MS analysis, the data nonetheless provide important information about the original sample composition. First, longer hydrogenation period (3000 min vs 1300 min) increases abundance of hydrofullerene fragments with lower carbon number (Figure 5). Second, the longer heating period also results in complete disappearance of $C_{60}H_x^+$ with the number of hydrogen atoms, $X < 28$. Finally, species with both even and odd numbers of carbon atoms are observed in the mass spectra, and the strongest overall signal is observed for $C_{59}H_x^+$ ions. Therefore, the C_2 loss mechanism typical for pure C_{60} is not observed exclusively in the mass spectra (Figure 3).

Notably, all observed fragmented fullerenes contain 22 or more hydrogen atoms. Hydrogen reaction with C_{60} occurs because of the opening of the C=C double bond, which results in formation of two C−H bonds. Therefore, only an even number of hydrogen atoms is expected in $C_{60}H_x$. Some low-abundance species with odd numbers of hydrogens likely result from deprotonation of hydrofullerene molecules during field desorption/ionization. We shall next discuss in more detail the two most important species, $C_{60}H_x$ and $C_{59}H_x$.

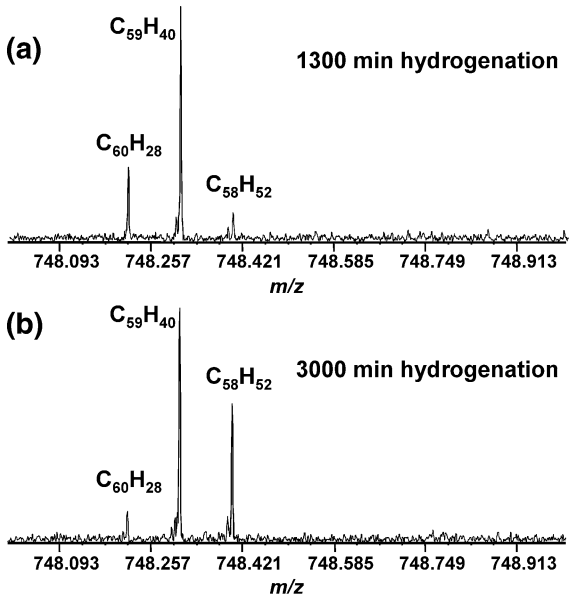

Figure 4. Expanded segment ($748 < m/z < 749$) of the FD FT-ICR mass spectra of hydrogenated fullerene samples (hydrogenated for (a) 1300 min and (b) 3000 min). The mass difference between neighboring monoisotopic peaks is ~94 mDa, corresponding to the mass difference between ^{12}C and $^1H_{12}$.

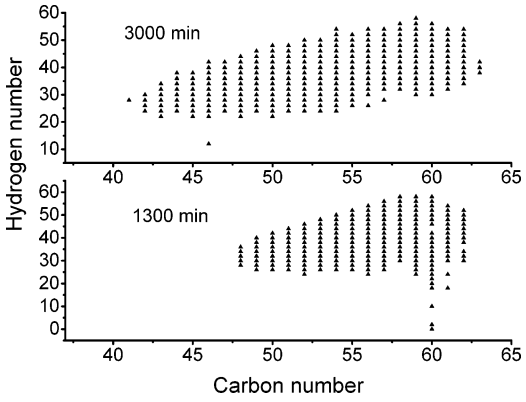

Figure 5. Elemental compositions of the components of the complex fullerene mixture shown in Figure 3b, c.

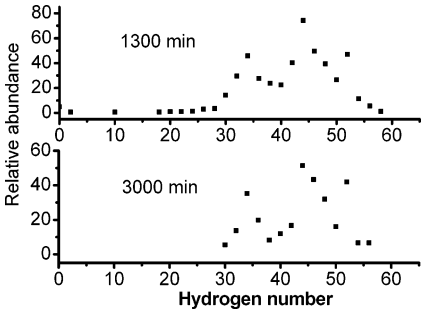

Figure 6. Relative abundances of $C_{60}H_x$ ions for the mass spectra of hydrogenated fullerene samples shown in Figure 3b, c.

$C_{60}H_x^+$ with $x > \sim 40$ as a Possible Source of Fragmentation in FT-ICR MS. Figure 6 shows the observed distribution of hydrogen for $C_{60}H_x^+$ ions. $C_{60}H_x^+$ ions with $X < 28$ are low in abundance for sample 1 and are absent altogether for sample 2. In both samples, peak distributions exhibit maxima correspond-

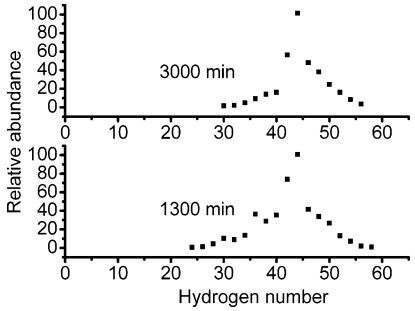

Figure 7. Relative abundances of $C_{59}H_x$ ions for the mass spectra of hydrogenated fullerene samples shown in Figure 3b, c.

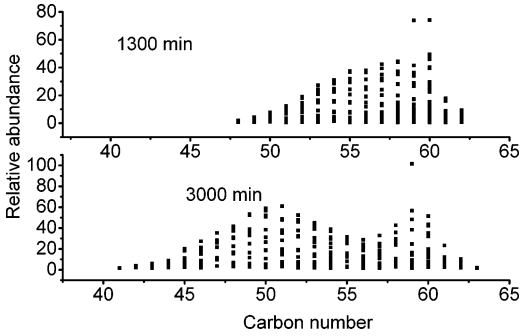

Figure 8. Relative abundances of hydrofullerene ions as a function of the number of carbon atoms, for the mass spectra shown in Figure 3b, c.

ing to $C_{60}H_{34}^+$, $C_{60}H_{44-46}^+$, and $C_{60}H_{52}^+$. The latter is particularly interesting because these highly hydrogenated species have not been observed as neutrals in the solid state. The most highly hydrogenated fullerenes seen here are $C_{60}H_{56}^+$ and $C_{60}H_{58}^+$. Such ions are generally considered unstable and corresponding peaks have thus far been interpreted as hydrofullerene oxides or trimethylene adducts when observed by low-resolution mass spectrometry.[6] On the basis of our analysis, the presence of trimethylene (C_3H_6) adducts was not confirmed. Furthermore, because additional hydrogenation cannot occur during MS analysis, these highly hydrogenated molecules ($C_{60}H_{52-58}^+$) must have been formed during the synthesis period by reaction of C_{60} and hydrogen gas. In addition, we observe a low abundance $C_{60-y}H_xO_z^+$, likely because of exposure of the samples to air. The radical cation of the commonly studied compound $C_{60}H_{36}$ is observed as a minor constituent of both samples, and hydrogenation of the present samples is more extensive than in previous reports.

Highly hydrogenated fullerenes are prime candidates for fragmentation both during synthesis ($C_{60}H_x$) and during MS experiments ($C_{60}H_x^+$). We therefore now compare peak distributions for $C_{60}H_x^+$ and $C_{59}H_x^+$ (the most abundant species observed by FD FT-ICR MS). The hydrogen number distribution for $C_{59}H_x^+$ ions (Figure 7) shows a maximum at 44 hydrogens for both samples. Ejection of CH from a $C_{60}H_x$ cage results in the formation of a seven- or eight-membered ring and dangling bond. If that fragmentation occurs during synthesis, in a high-pressure hydrogen atmosphere, the dangling bond will be immediately saturated with a hydrogen atom and the net change will be a loss of exactly one carbon atom (e.g., $C_{60}H_{44} \rightarrow C_{59}H_{44}$). If CH ejection occurs during FD FT-ICR mass analysis experiment, the absence of hydrogen will result in a transformation of the type $C_{60}H_{44}^+ \rightarrow C_{59}H_{43}^+$. The dominant presence of $C_{59}H_{44}^+$ in our mass spectra supports hydrofullerene fragmentation during synthesis: an odd hydrogen number of hydrofullerene molecules, such as $C_{60}H_{45}$, cannot be synthesized during hydrogenation. This conclusion supports our prior MALDI TOF MS results,[21] which suggested that sample 2 was composed predominantly of fragmented fullerenes based on C_{58} and C_{59} cages.[21] Because of defective cage structure, these hydrofullerenes are likely less stable than $C_{60}H_x$, thereby accounting for their facile fragmentation during MS analysis.

$C_{59}H_x$ as a Possible Source of Fragmentation in FT-ICR MS. Figure 8 shows the relative abundance of all hydrofullerene species observed in the present samples. The most abundant species in sample 1 are $C_{60}H_x^+$ and $C_{59}H_y^+$ with a monotonic decrease in abundance with a decreasing number of carbon atoms (Figure 8, top). On the basis of Figure 6 and Figure 7, the most abundant ions in the $C_{60}H_x^+$ and $C_{59}H_y^+$ families are $C_{60}H_{44}^+$ and $C_{59}H_{44}^+$. Therefore, $C_{59}H_{44}^+$ is a likely prime candidate for fragmentation in FT-ICR MS experiments because of its high relative abundance and lower stability relative to $C_{60}H_x^+$ hydrofullerenes.

According to the proposed model, the loss of one carbon atom from $C_{60}H_{44}$ with formation of $C_{59}H_{44}$ occurs during synthesis and most other fragmentation occurs during ionization or other gas-phase manipulation during FD FT-ICR MS. Sample 2 shows a decrease in the abundance of $C_{60}H_x^+$ while the abundance of $C_{59}H_y^+$ increases. Thus, the main source of fragmentation in the MS experiments is $C_{59}H_y^+$. The instability of $C_{59}H_{44}$ molecules (and presumably of $C_{59}H_{44}^+$ ions) leads to a bimodal abundance distribution with a second maximum centered at $C_{52}H_x^+$ and $C_{50}H_x^+$, Figure 8, bottom), indicating that the $C_{52}H_x^+$ and $C_{50}H_x^+$ hydrofullerenes are more stable than $C_{59}H_{44}^+$. Otherwise, the abundances of smaller hydrofullerenes would decline with decreasing carbon number without a local minimum. An alternative explanation is that the cage structure partly collapses when the molecule becomes too small, and $C_{50-52}H_x^+$ molecules are not fullerenes.

Possible Fragmentation Pathways. In summary, hydrogenation of C_{60} at elevated H_2 pressure and temperature leads to formation of hydrofullerenes $C_{60}H_x$ with high hydrogen content ($X > 40$). These hydrofullerenes are unstable under the synthesis conditions, and on prolonged exposure to hydrogen gas at high temperature, they start to fragment by ejection of mostly CH units to yield $C_{59}H_x$, $C_{58}H_x$, and so forth. Dangling bonds resulting from such ejection are promptly saturated by hydrogen atoms to stabilize the overall molecular structure. During subsequent FD ionization and FT-ICR MS analysis, both $C_{60}H_x^+$ ($X > 40$) and $C_{60-y}H_x^+$ ($Y = 1-4$, $X > 40$) undergo fragmentation by loss of C_2H_2 units. This model is supported by examination of the most abundant ions from each set of C_yH_x ($Y = 60-43$) in the mass spectrum of the sample hydrogenated for 3000 min (Figure 9).

Our data suggest that the most abundant hydrofullerene ions originate from the most abundant corresponding neutrals in the synthesized mixture and their gas-phase produced fragments. For example, the most abundant among $C_{60}H_x^+$ hydrofullerenes is $C_{60}H_{44}^+$. The most abundant species in the $C_{56-59}H_x^+$ family all have $X = 44$, presumably derived from sequential CH losses (each accompanied by subsequent addition of H, for a net loss of one carbon atom) from $C_{60}H_{44}$ during synthesis.

Figure 9 shows possible fragmentation pathways for the initially most abundant hydrofullerene ions; arrows correspond to the loss of C_2H_2 units. The longest reaction chain starts from $C_{60}H_{44}^+$. However, abundances of the compounds for the first two to three fragmentation stages are not as high as those originating from, for example, $C_{59}H_{44}^+$. The fullerene molecules with "defective" structures (i.e., C_{60} minus one or a few carbon atoms) are less symmetrical and presumably less stable. Therefore, fragmentation of $C_{60-y}H_x$ is likely to be more

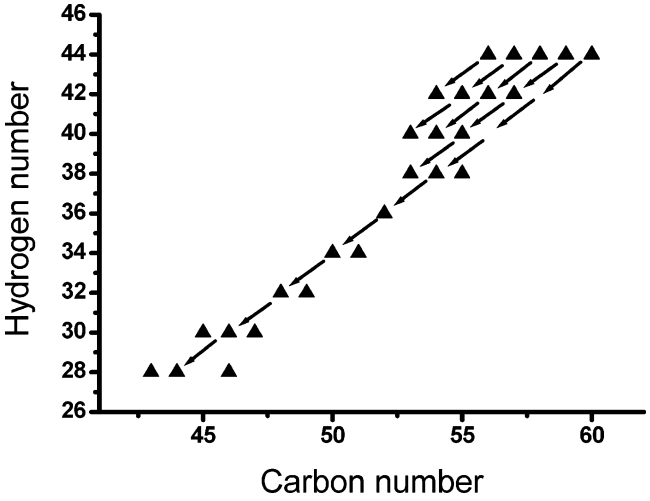

Figure 9. Most abundant ions in the FD FT-ICR mass spectrum of the sample hydrogenated for 3000 min. If two or three ion abundances were nearly the same, all of them are shown.

pronounced. Also, it is possible that some molecules collapse during the first steps of fragmentation, so that fragments from "defective" hydrofullerenes become less abundant with a decreasing number of carbon atoms in the cage. The series of $C_{60}H_{44}^+$ fragments is longer, and for carbon numbers below 53, the most abundant species are those that originate from $C_{60}H_{44}^+$. Finally, the data shown in Figure 9 confirm that not only $C_{60}H_x$ but also $C_{59}H_x$, $C_{58}H_x$, $C_{57}H_x$, and $C_{56}H_x$ are present in the sample after synthesis and prior to mass spectrometry.

Conclusions

The data presented in this study can be explained by two fragmentation mechanisms. The first mechanism is responsible for formation of $C_{59}H_x$ and $C_{58}H_x$ in bulk amount during prolonged hydrogenation of C_{60}, whereas secondary gas-phase fragmentation processes during MS analysis probably produce most of the hydrofullerene ions with smaller numbers of carbon atoms. Nevertheless, we observe that most abundant products of the prolonged hydrogenation of C_{60} are $C_{59}H_x$ and $C_{58}H_x$ (which compose a significant part of the sample hydrogenated for 3000 min). Although it is difficult to estimate quantitatively the yield of $C_{59}H_x$ for these samples because of the complex nature of the obtained hydrofullerene mixtures, the issue might be resolved by combination of liquid chromatography and high-resolution mass spectrometry.

Acknowledgment. This work was supported by the NSF National High Field FT-ICR Facility (CHE-99-09502), Florida State University, and the National High Magnetic Field Laboratory in Tallahassee, FL. Y.M.S. thanks RFBR for support (project 00-03-32796). Part of the work was financially supported by the Swedish Research Council.

Note Added after ASAP Publication. This article was published ASAP on June 15, 2005. References 15 and 23 were corrected. The correct version was reposted on June 22, 2005.

References and Notes

(1) Breda, N.; Broglia, R. A.; Colo, G.; Onida, G.; Provasi, D.; Vigezzi, E. *Phys. Rev. B* **2000**, *62*, 130−133.
(2) Romero, N. A.; Kim, J.; Martin, R. M. *Phys. Rev. B* **2004**, *70*.
(3) Prinzbach, H.; Weller, A.; Landenberger, P.; Wahl, F.; Worth, J.; Scott, L. T.; Gelmont, M.; Olevano, D.; von Issendorff, B. *Nature* **2000**, *407*, 60−63.
(4) Xie, S. Y.; Gao, F.; Lu, X.; Huang, R. B.; Wang, C. R.; Zhang, X.; Liu, M. L.; Deng, S. L.; Zheng, L. S. *Science* **2004**, *304*, 699−699.
(5) Marques, L.; Hodeau, J. L.; NunezRegueiro, M.; Perroux, M. *Phys. Rev. B* **1996**, *54*, 12633−12636.
(6) Darwish, A. D.; AbdulSada, A. K.; Langley, G. J.; Kroto, H. W.; Taylor, R.; Walton, D. R. M. *Synth. Met.* **1996**, *77*, 303−307.
(7) Ruchardt, C.; Gerst, M.; Ebenhoch, J.; Beckhaus, H. D.; Campbell, E. E. B.; Tellgmann, R.; Schwarz, H.; Weiske, T.; Pitter, S. *Angew. Chem., Int. Ed. Engl.* **1993**, *32*, 584−586.
(8) Kolesnikov, A. I.; Antonov, V. E.; Bashkin, I. O.; Grosse, G.; Moravsky, A. P.; Muzychka, A. Y.; Ponyatovsky, E. G.; Wagner, F. E. *J. Phys.: Condens. Matter* **1997**, *9*, 2831−2838.
(9) Peera, A. A.; Alemany, L. B.; Billups, W. E. *Appl. Phys. A* **2004**, *78*, 995−1000.
(10) Attalla, M. I.; Vassallo, A. M.; Tattam, B. N.; Hanna, J. V. *J. Phys. Chem.* **1993**, *97*, 6329−6331.
(11) Dorozhko, P. A.; Lobach, A. S.; Popov, A. A.; Senyavin, V. M.; Korobov, M. V. *Chem. Phys. Lett.* **2001**, *336*, 39−46.
(12) Shul'ga, Y. M.; Tarasov, B. P.; Fokin, V. M.; Shul'ga, N. Y.; Vasilets, V. N. *Phys. Solid State* **1999**, *41*, 1391−1397.
(13) Okotrub, A. V.; Bulusheva, L. G.; Asanov, I. P.; Lobach, A. S.; Shulga, Y. M. *J. Phys. Chem. A* **1999**, *103*, 716−720.
(14) Nossal, J.; Saini, R. K.; Sadana, A. K.; Bettinger, H. F.; Alemany, L. B.; Scuseria, G. E.; Billups, W. E.; Saunders, M.; Khong, A.; Weisemann, R. *J. Am. Chem. Soc.* **2001**, *123*, 8482−8495.
(15) Loufty, R. O.; Wexler, E. M. *Feasibility of Fullerene Hydride as a High Capacity Hydrogen Storage Material*; NREL/CP-570-30535; 2001 (http://www.eere.energy.gov/hydrogenandfuelcells/pdfs/30535al.pdf).
(16) Tarasov, B. P.; Shul'ga, Y. M.; Fokin, V. N.; Vasilets, V. N.; Shul'ga, N. Y.; Schur, D. V.; Yartys, V. A. *J. Alloys Compd.* **2001**, *314*, 296−300.
(17) Shul'ga, Y. M.; Tarasov, B. P.; Fokin, V. N.; Martynenko, V. M.; Schur, D. V.; Volkov, G. A.; Rubtsov, V. I.; Krasochka, G. A.; Chapusheva, N. V.; Shevchenko, V. V. *Carbon* **2003**, *41*, 1365−1368.
(18) Darwish, A. D.; Avent, A. G.; Taylor, R.; Walton, D. R. M. *J. Chem. Soc., Perkin Trans. 2* **1996**, 2051−2054.
(19) Talyzin, A. V.; Shulga, Y. M.; Jacob, A. *Appl. Phys. A* **2004**, *78*, 1005−1010.
(20) Talyzin, A. V.; Sundqvist, B.; Shulga, Y. M.; Peera, A. A.; Imus, P.; Billups, W. E. *Chem. Phys. Lett.* **2004**, *400*, 112−116.
(21) Talyzin, A. V.; Tsybin, Y. O.; Peera, A. A.; Schaub, T. M.; Marshall, A. G.; Sundqvist, B.; Mauron, P.; Zuttel, A.; Billups, W. E. *J. Phys. Chem. B* **2005**, *109*, 5403−5405.
(22) Schaub, T. M.; Hendrickson, C. L.; Qian, K. N.; Quinn, J. P.; Marshall, A. G. *Anal. Chem.* **2003**, *75*, 2172−2176.
(23) Schaub, T. M.; Hendrickson, C. L.; Quinn, J. P.; Rodgers, R. P.; Marshall, A. G. *Anal. Chem.* **2005**, *77*, 1317−1324.
(24) Hathiramani, D.; Aichele, K.; Arnold, W.; Huber, K.; Salzborn, E.; Scheier, P. *Phys. Rev. Lett.* **2000**, *85*, 3604−3607.
(25) Nakai, Y.; Kambara, T.; Itoh, A.; Tsuchida, H.; Yamazaki, Y. *Phys. Rev. A* **2001**, *6404*, art. no.-043205.
(26) Dunser, B.; Echt, O.; Scheier, P.; Mark, T. D. *Phys. Rev. Lett.* **1997**, *79*, 3861−3864.
(27) Ryabenko, A. G.; Muradyan, V. E.; Esipov, S. E.; Cherepanova, N. I. *Russ. Chem. Bull.* **2003**, *52*, 1516−1521.
(28) Heiney, P. A.; Fischer, J. E.; McGhie, A. R.; Romanow, W. J.; Denenstein, A. M.; McCauley, J. P.; Smith, A. B.; Cox, D. E. *Phys. Rev. Lett.* **1991**, *66*, 2911−2914.
(29) Hall, L. E.; McKenzie, D. R.; Davis, R. L.; Attalla, M. I.; Vassallo, A. M. *Acta Crystallogr., Sect. B* **1998**, *54*, 345−350.
(30) Meletov, K. P.; Tsilika, I.; Assimopoulos, S.; Kourouklis, G. A.; Ves, S.; Bashkin, I. O.; Kulakov, V. L.; Khasanov, S. S. *Phys. Status Solidi B* **2001**, *223*, 459−467.